J Appl Physiol 103: 796–802, 2007.
First published May 17, 2007; doi:10.1152/japplphysiol.01451.2006.

Motor unit composition has little effect on the short-range stiffness of feline medial gastrocnemius muscle

Lei Cui,[1] Eric J. Perreault,[1,2] and Thomas G. Sandercock[3]

Departments of [1]Biomedical Engineering, [2]Physical Medicine and Rehabilitation, and [3]Physiology, Northwestern University, Chicago, Illinois

Submitted 22 December 2006; accepted in final form 17 May 2007

Cui L, Perreault EJ, Sandercock TG. Motor unit composition has little effect on the short-range stiffness of feline medial gastrocnemius muscle. *J Appl Physiol* 103: 796–802, 2007. First published May 17, 2007; doi:10.1152/japplphysiol.01451.2006.—Studies on skinned fibers and single motor units have indicated that slow-twitch fibers are stiffer than fast-twitch fibers. This suggests that skeletal muscles with different motor unit compositions may have different short-range stiffness (SRS) properties. Furthermore, the natural recruitment of slow before fast motor units may result in an SRS-force profile that is different from electrical stimulation. However, muscle architecture and the mechanical properties of surrounding tissues also contribute to the net SRS of a muscle, and it remains unclear how these structural features each contribute to the SRS of a muscle. In this study, the SRS-force characteristics of cat medial gastrocnemius muscle were measured during natural activation using the crossed-extension reflex, which activates slow before fast motor units, and during electrical activation, in which all motor units are activated synchronously. Short, rapid, isovelocity stretches were applied using a linear puller to measure SRS across the range of muscle forces. Data were collected from eight animals. Although there was a trend toward greater stiffness during natural activation, this trend was small and not statistically significant across the population of animals tested. A simple model, in which the slow-twitch fibers were assumed to be 30% stiffer than the fast-twitch fibers, was used to simulate the experimental results. Experimental and simulated results show that motor unit composition or firing rate has little effect on the SRS property of the cat MG muscle, suggesting that architectural features may be the primary determinant of SRS.

architecture; passive tissues; firing rate

PERTURBING AN ACTIVE MUSCLE with short quick stretches or releases produces transient changes in force very similar to those obtained from a simple spring: the change in muscle force is proportional to the change in muscle length. This behavior is believed to result from attached cross bridges in the muscle, as well as the material properties of the tendon and aponeurosis. This property is often referred to as short-range stiffness (SRS). Larger or longer movements produce much more complex responses because of the dynamics of cross-bridge cycling (9, 13, 22), but SRS is considered important for the control of posture, because it determines the initial response of a muscle to imposed disturbances before reflexes or voluntary interventions can alter activation. Understanding how muscle structure contributes to whole muscle SRS is important for assessing how structurally distinct muscles can contribute to the stiffness and stability properties of a whole limb. The goal of this work was to assess the contributions of muscle fiber composition to SRS.

SRS increases monotonically with force (7, 8, 10, 15). This increase is typically linear at low force levels and less than linear at higher force levels, resulting in a concave SRS-force relationship. This concave relationship is due, at least in part, to the serial connection of the muscle fibers with the aponeurosis and external tendon. The net SRS of a muscle is dominated by the least stiff element in this serial linkage. If it is assumed that the SRS of the tendon and aponeurosis is constant at all muscle forces, an approximation that is certainly incorrect at very low force, and that the SRS of the active muscle fibers is linearly proportional to muscle force, then the net SRS will be dominated by the muscle fiber stiffness at low force levels and by the stiffness of the connective tissues at higher forces. This results in the concave SRS-force relationship described well by Morgan (15). The degree of concavity for a specific muscle will depend on the relative stiffness of its maximally activated fibers and its tendinous structures.

The architectural features of the fibers within a muscle can contribute to the differences in SRS across muscles. SRS is inversely related to fascicle length, since the stiffness of serially connected sarcomeres adds reciprocally. The elegant results of Walmsley and Proske (29) suggest that differences in fiber length between the cat soleus and medial gastrocnemius (MG) muscles account for most of the differences in SRS between these muscles. The number of fibers in a muscle also will influence the maximum SRS that can be obtained, since the stiffnesses of fibers connected in parallel add linearly. Finally, pennation angles also should impact muscle fiber contributions to SRS properties within individual muscles and across muscles; however, this theory has not been tested experimentally.

The composition of fiber types within a muscle may contribute to the concave SRS-force relationship. Studies on isolated muscle fibers have shown lower SRS in fast-twitch type II than in slow-twitch type I fibers (14), and similar conclusions have been reached for single motor units (17, 21). During natural activation, where slow motor units are recruited before faster units, these differences in stiffness between motor unit types also could contribute to the concave SRS-force relationship. These differences, however, have not been observed at the whole muscle level (8). Nevertheless, these studies have focused on fiber type contributions across muscles, where additional differences in muscle structure may obscure any differences due to fiber type. Furthermore, results in amphibian muscle suggest that there may not be a difference in SRS with

Address for reprint requests and other correspondence: T. Sandercock, Dept. of Physiology, M211, Ward 5-295, Northwestern Univ., Feinberg School of Medicine, 303 E. Chicago Ave., Chicago, IL 60611 (e-mail: t-sandercock@northwestern.edu).

The costs of publication of this article were defrayed in part by the payment of page charges. The article must therefore be hereby marked "*advertisement*" in accordance with 18 U.S.C. Section 1734 solely to indicate this fact.

fiber type. Gregory et al. (6) showed that, when normalized by sarcomere number, stiffness of slow- and fast-twitch fibers tends to be similar, provided the stretch of fast-twitch fibers is sufficient to prevent cross-bridge breakage.

One example of a structural difference that could mask fiber type contributions to SRS is the difference in the contributions of the tendon and aponeurosis across muscles. The nonlinear material properties of the tendon may affect the slope of the SRS-force relationship at different force levels (20), since excised tendon has been shown to be less stiff at low forces (2, 18). These contributions would be most significant at lower force levels, where differences in fiber type across muscles also would be expected to most significantly alter the SRS-force relationship.

The purpose of this study was to quantify how muscle fiber type and firing rate contribute to the SRS properties of a muscle. To control for the range of architectural features that can influence SRS, all statistical comparisons were made within the same muscle. The cat MG muscle, which contains ~75% fast-twitch fibers and 25% slow-twitch fibers (1), was used in all experiments; the slow-twitch fibers occupy ~14% of the cross-sectional area of the muscle (3). The population of active fibers was controlled using natural and electrical activation protocols. Natural recruitment via the crossed-extension (CX) reflex was used to preferentially recruit slow- before fast-twitch fibers; electrical stimulation was used to alter the natural recruitment order by activating the slow- and fast-twitch fibers synchronously. The null hypothesis was that there would be no difference in the SRS-force relationships measured using these different activation protocols. A significant difference in SRS between the naturally and electrically activated muscles would provide direct evidence for significant fiber type contributions to whole muscle SRS.

METHODS

Surgical procedure. Experiments were performed on eight cats. All procedures were approved by the Animal Care Committee of Northwestern University and conformed to policies established by the National Institutes of Health. Initial surgical preparations were done under deep gaseous anesthesia (1.5–3.0% isoflurane in 3:1 O_2-NO_2) according to standard procedures in our laboratory (24). The MG muscle of the left hindlimb was isolated from the surrounding tissues, with care taken to preserve the innervation and blood supply. The calcaneus was cut to allow secure attachment to the testing apparatus. A combination of mineral oil-soaked cotton and mineral oil pools formed within pulled-up skin flaps was used to maintain moisture in exposed areas.

For CX protocols, reflexes must remain strong. Therefore, a precollicular decerebration was performed so that the CX trials could be conducted without chemical anesthesia, which suppresses reflex activity. The midbrain was transected with an ophthalmic spatula, the entire forebrain was aspirated, and the calvarium was packed with saline-soaked cotton wool. The gaseous anesthesia was then discontinued, and the animal was allowed to breathe room air. Under these conditions, pressure on the contralateral leg activates the MG muscle via the CX reflex.

After the CX trials, the spinal cord was prepared to allow direct stimulation of the ventral roots. Pentobarbital sodium was administered intravenously to minimize reflexes during surgery. A laminectomy of the spinal column was performed from L_4 to S_1. Ipsilateral dorsal roots from L_4 to S_2 were transected to eliminate reflexes. The ventral roots (L_7 and/or S_1, depending on the innervation to the MG muscle) were divided into four to six bundles, so that each bundle produced a similar amount of force for use with the rate-coding (RA) protocol (see below); combinations of bundles were used to produce a range of forces during the recruitment (RE) protocol. Radiant heat was used to maintain hindlimb, spinal cord, and core temperatures within physiological limits.

Experimental protocols. For estimation of the optimum length of the muscle (L_o), the passive tension was measured at a range of muscle lengths. On the basis of our experience, ~2–3 N of passive tension is generated at L_o for the MG muscle. L_o was confirmed at the end of each experiment by measurement of the length-tension relationship. This procedure resulted in all stiffness measurements being made within ±2 mm of L_o. Since active SRS is independent of muscle length (15), our measurements were not sensitive to these small variations.

SRS was measured using ramp displacements of muscle length. Length was controlled using a linear motor (ThrustTube TB3806, Copley Controls, Canton, MA) configured as a stiff position servo (~250 N/mm). This device was instrumented to measure muscle length (model RGH24, Renishaw, Gloucestershire, UK) and force (model 31, Honeywell Sensotec, Columbus, OH). Each imposed displacement had an amplitude of 2 mm and a velocity of 200 mm/s. Length changes were imposed only after muscle force had reached a steady level.

Stiffness measurements were made during three different muscle activation protocols. We first used the CX reflex to generate natural patterns of motor unit recruitment and rate modulation (4) (Fig. 1*A*). This reflex was elicited by mechanical stimulation of the contralateral hindlimb; different levels of mechanical stimulation were used to grade muscle force. Once a desired level of force was reached, the muscle stretch was initiated. In addition to the CX reflex, two electrical stimulation protocols were used to determine whether SRS was influenced only by muscle force or also by the firing rate and number of active motor units (Fig. 1*B*). The RA protocol involved simultaneous, interleaved stimulation of all dissected ventral root bundles; force was varied by grading the stimulation frequency of each bundle from 20 to 100 Hz. This paradigm is similar to that used previously by Rack and Westbury (22). For the final activation protocol, RE, electrically stimulated ventral roots were recruited. Active roots were stimulated using constant-frequency 100-Hz pulse trains; force was graded by varying the number and combination of ventral root bundles that were stimulated. In both electrical stimulation protocols, the duration of the stimulation pulse trains was 0.5 s, and muscle stretch was initiated 0.4 s after stimulation onset. In all protocols, each active trial was followed by a passive trial; a 60-s rest period was imposed between all trials to minimize muscle fatigue, which was monitored by replication and comparison of trials throughout the experiment. The RA protocol was successfully conducted in all eight cats, whereas useful stiffness measurements were obtained from six cats with the CX protocol and from seven cats the RE protocol.

Data analysis. For determination of SRS, the slope of the force-length trajectory was calculated from data collected during the constant-velocity portion of the applied perturbation, which began ~1 ms after the onset of perturbation. Only 5 ms of data were used in the subsequent analysis to avoid forces related to reflex activation. This criterion also allowed measurements to be made before the onset of yielding (Fig. 2). In the CX protocols, only data with a steady background force (peak-to-peak force variation was <10% of average force) within the 100 ms before perturbation onset were used to calculate SRS to minimize the effect of changes in cross-bridge cycling rate on SRS. This criterion also was met in the electrical stimulation protocols, except at stimulation frequencies below ~30 Hz.

An elastic model (*Eq. 1*), initially proposed by Morgan (15), was used to describe the relationship between SRS and muscle force. The model used in the present study is identical to that proposed by Morgan, except it is formulated in terms of stiffnesses, rather than compliances, for a more direct comparison with our measured vari-

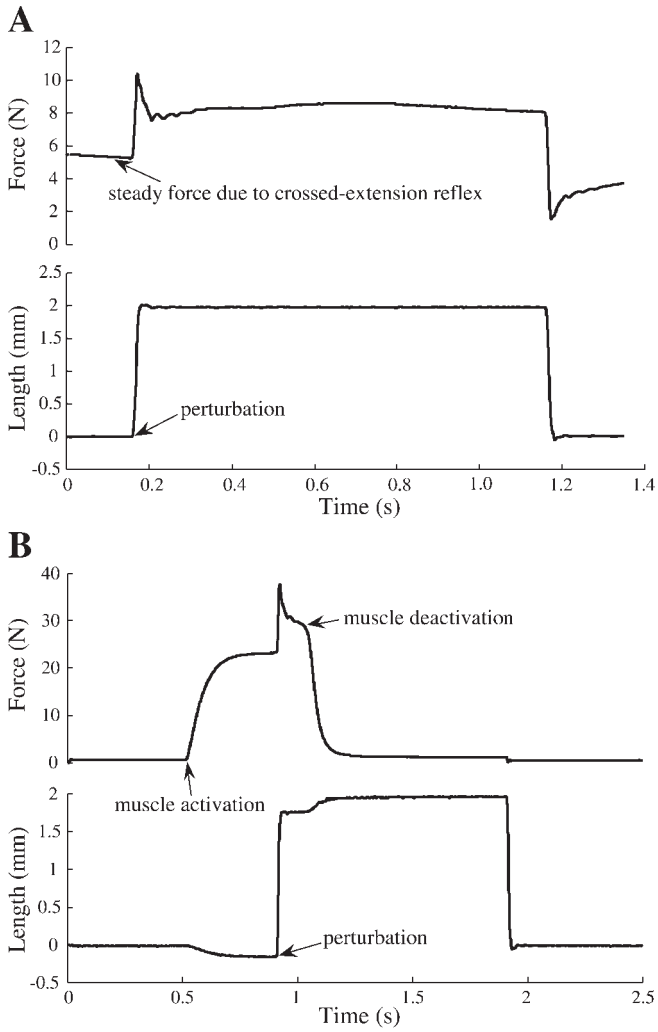

Fig. 1. Stiffness measurement protocols. *A*: crossed-extension (CX). Muscle force due to CX reflex reached a steady state before application of perturbation. *B*: direct stimulation [rate coding (RA) and recruitment (RE) protocols]. Slight muscle shortening due to activation and lengthening due to deactivation can be observed on the length trace. In both cases, zero muscle length corresponds to muscle length before perturbation, i.e., the optimum length.

ables. The main assumption of this model is that SRS within the active muscle fibers is proportional to the number of cross bridges attached and, therefore, increases with muscle force. Another important assumption is that all passive elasticity is connected in series with the muscle fibers and is independent of muscle force. Although it is highly simplified, this model provides a good estimate of the SRS-force relationship (15). The formulation is given in *Eq. 1*

$$SRS = \beta P \cdot K_T/(\beta P + K_T) \quad (1)$$

where P is muscle force, K_T is the tendon stiffness (N/mm), and β is a constant (mm^{-1}) representative of the active muscle stiffness per unit muscle force. This parameter is dependent on cross-bridge stiffness and is referred to as the normalized active muscle stiffness. Through this relationship, the total stiffness can be divided into an active component (βP) and a passive component (K_T).

Model parameters and confidence intervals were estimated using a Gauss-Newton algorithm in Matlab (Mathworks, Natick, MA). The constraints shown in *Eq. 2* were used to ensure that the SRS for each model was identical at the maximal obtainable muscle force, even though this force could not be reached in the CX experiments

$$SRS_{CX}(P_o) = SRS_{RA}(P_o); \quad SRS_{RE}(P_o) = SRS_{RA}(P_o) \quad (2)$$

where P_o is the optimum force, and the subscripts refer to the three activation protocols. With these constraints, only four parameters were needed to fit the data from each cat across all three protocols. The influence of these parameters on the SRS was examined using a sensitivity analysis computed directly from *Eq. 1*, according to the relationship shown in *Eq. 3*, where S_x is sensitivity to a given parameter *x*.

$$S_x = \frac{\partial SRS/\partial x}{SRS/x} \quad (3)$$

To test our null hypothesis that the SRS-force relationships of different activation methods are not significantly different, we chose the parameter β for statistical comparisons across the activation protocols, since this represents the net active muscle contribution to the net SRS. A significant difference in β would indicate that the activation protocol and, hence, the muscle fiber type or the firing rate have a significant effect on the SRS-force relationship for the whole muscle. Comparisons were made using a general linear model, with activation modeled as a fixed factor and each animal as a random factor. All statistical analyses were conducted in R (21a).

The above-mentioned model, used to describe the experimental data, was extended to evaluate the effect of motor unit recruitment order on SRS of muscles with connective tissue properties and motor unit compositions different from those of the MG muscle. It was

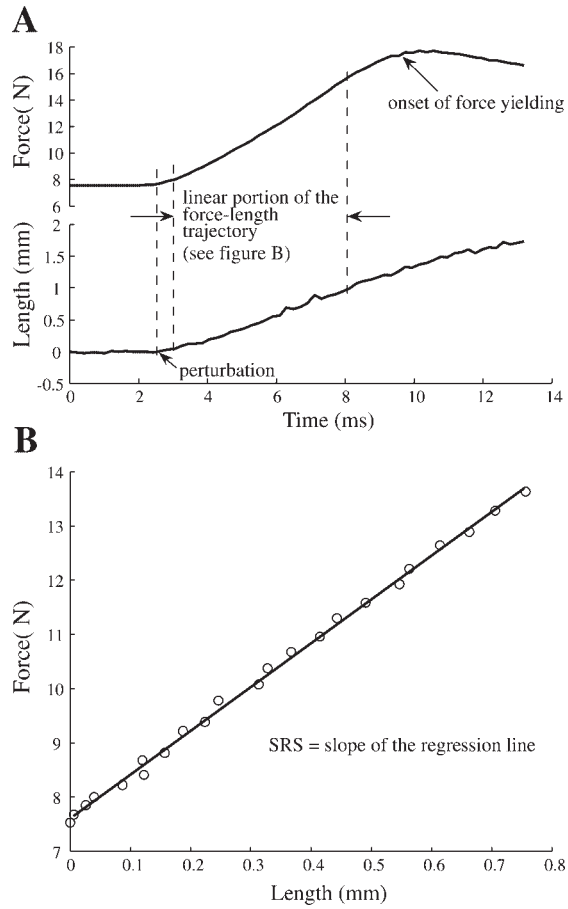

Fig. 2. Calculation of short-range stiffness (SRS). *A*: muscle force and length as a function of time during perturbation. Linear portion of the force-length trajectory was used for SRS calculation. *B*: linear regression of force-length data of the linear portion.

assumed that the slow-twitch fibers are ~30% stiffer than the fast-twitch fibers (14). The extended model is shown in *Eq. 4*

$$SRS = \frac{[\beta_S \cdot P_S + \beta_F \cdot (1 - P_S)] \cdot P \cdot (R_K \cdot K_M)}{[\beta_S \cdot P_S + \beta_F \cdot (1 - P_S)] \cdot P + (R_K \cdot K_M)} \quad (4)$$

where β_S and β_F are the β parameters for slow- and fast-twitch fibers, respectively ($\beta_S = 1.3\beta_F$) (14); P_S is the percentage of total force generated by slow-twitch fibers; K_M is the maximum muscle fiber stiffness, i.e., when the muscle is fully activated; and R_K is the ratio of K_T to K_M. In CX experiments, it was assumed that all slow-twitch fibers were recruited before any fast-twitch fibers were recruited; in RA experiments, however, slow-twitch fibers were recruited simultaneously with fast-twitch fibers according to the proportion of force generated by each fiber type; this assumption for recruitment order for CX experiments was chosen to exaggerate any contribution due to fiber-specific differences in SRS.

R_K was chosen to range from 0.2 (very compliant tendon) to 100 (very stiff tendon). For comparison, this parameter is ~0.5 for the cat MG muscle on the basis of our experimental data. For each combination of R_K and P_S ($0 \leq P_S \leq 1$), normalized muscle SRS as a function of normalized force was calculated. The maximum difference (ΔSRS_{max}) between values from CX and RA experiments normalized by the maximum SRS was then compared for each combination of R_K and P_S.

RESULTS

The SRS model described in *Eq. 1* fit the data well for all animals. The average r^2 value across all animals and all stimulation protocols was 0.98 ± 0.01 (mean ± SD). In addition, the estimated normalized active stiffness, β, had an average coefficient of variation of only 8 ± 3%.

There was substantial overlap in the normalized active stiffness estimated across the different activation protocols. Figure 3 shows the SRS data and the model fits for a single representative animal. For these data, there was no statistically significant difference in the β values estimated from data collected during the two electrical stimulation protocols ($P > 0.05$) and a small but statistically significant increase ($P < 0.01$) in the β values estimated from the data collected during the CX protocol.

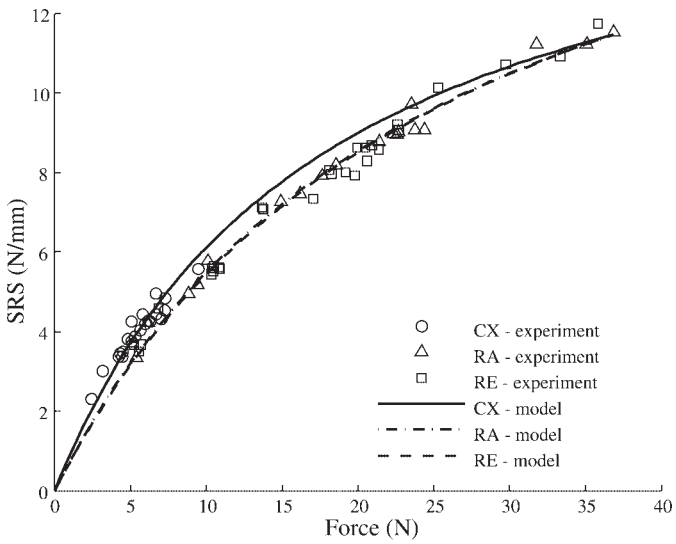

Fig. 3. Typical SRS-force relationships measured during CX, RA, and RE activation protocols in a single animal. SRS-to-force ratio was significantly higher in the CX protocol (0.95 ± 0.05) than in the RA (0.77 ± 0.05) and RE (0.75 ± 0.03) protocols.

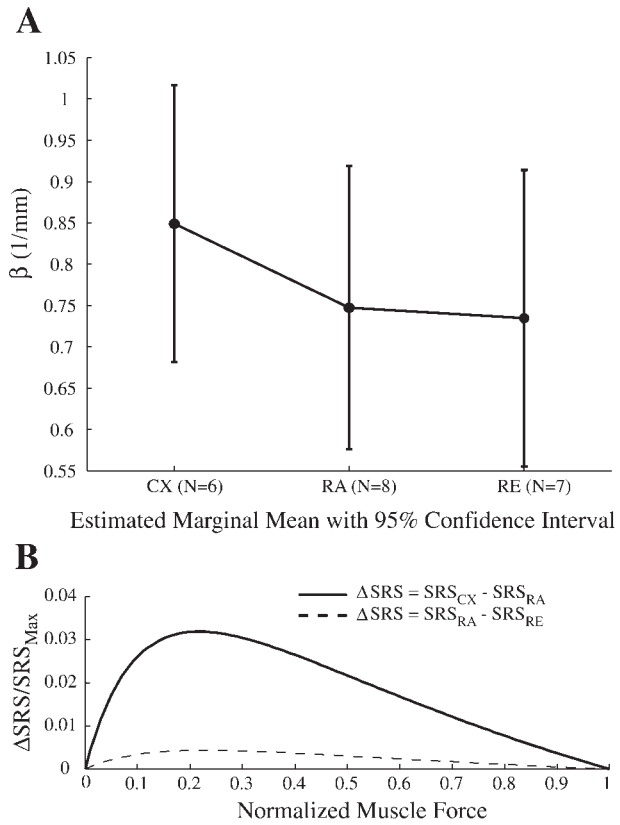

Fig. 4. Group results for the influence of the activation protocols on SRS. *A*: normalized SRS (β) measured during each protocol. Results are modeled population responses and associated 95% confidence intervals. *B*: difference in SRS across the full range of muscle forces. Results are expressed as percentage of SRS measured at maximal muscle force and calculated using parameters estimated from group data.

Across the group of animals tested, there was no statistically significant difference in the β values estimated for the three activation protocols ($P > 0.3$). The average group results are illustrated in Fig. 4*A*. Of the six animals that completed the CX protocol, β_{CX} values were significantly greater than β_{RE} and β_{RA} values in three cats, significantly lower than β_{RE} and β_{RA} values in one cat, and not significantly different from β_{RE} and β_{RA} values in two cats. There was no significant difference in the estimated β_{RE} and β_{RA} parameters in five of the seven animals that completed these two protocols; β_{RE} was significantly larger than β_{RA} in one of the remaining animals and significantly smaller in the other. Although no statistically significant differences were observed in the SRS measured during the three activation protocols, there was a trend toward slightly increased stiffness during the CX protocol. Figure 4*B* illustrates how this small increase contributed to the difference in the SRS measured in the three activation protocols across the full range of muscle forces. The largest differences occurred at <25% of maximum muscle force and remained <4% of the SRS measured at maximal muscle activation. Together, these results demonstrate that, of the three protocols tested, the CX protocol has the largest influence on whole muscle SRS, but this influence is small.

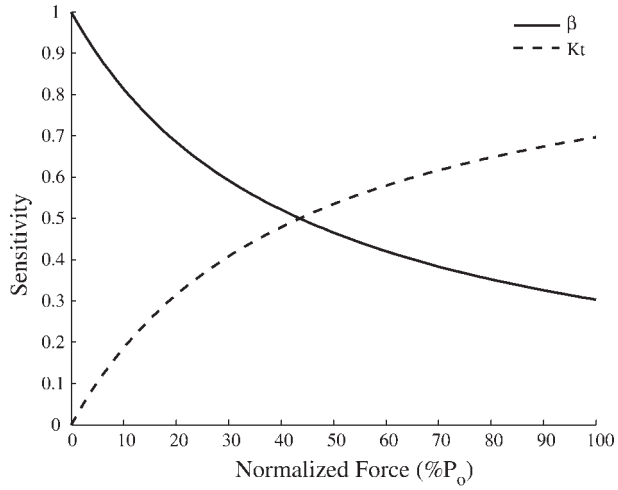

Fig. 5. Sensitivity plot of β and tendon stiffness (K_T) based on average model parameters of all animals from CX protocols. P_o, optimum force.

For cat MG muscle, active stiffness from the muscle fibers dominates the net SRS below ~40% of maximal muscle force. Above this point, stiffness from the tendinous components becomes the dominant contributor to whole muscle SRS. We used the group parameters measured during the CX protocol to calculate the sensitivity of SRS to β and K_T (Fig. 5).

The modified model (*Eq. 4*) simulation results are shown in Fig. 6. The normalized SRS as a function of normalized force for the MG muscle ($P_S = 0.14$, $R_K = 0.5$) is shown in Fig. 6*A*. The maximum difference between the CX and RA protocols occurs at 14% of the total force and is <7% of the maximum SRS. The normalized ΔSRS as a function of force for multiple stiffness ratios R_K when $P_S = 0.14$ is shown in Fig. 6*B*. The vertical line in Fig. 6*B* connects the maxima of all curves. All occurred at the same normalized muscle force, which was equal to P_S ($P_S = 0.14$ in this case). The discontinuous nature of these curves resulted from our simplified RE model, which was chosen to accentuate fiber-dependent stiffness contributions to whole muscle SRS. Figure 6*C* shows the normalized ΔSRS_{max} for the range of R_K and P_S tested. For reference, the maxima from Fig. 6*B* are indicated by the vertical line and the associated intersection points. The normalized ΔSRS_{max} is <7% for all cases.

DISCUSSION

The effect of motor unit recruitment was examined directly by comparing the SRS-force relationship between naturally recruited motor units, activated via the CX reflex, and electrically stimulated motor units. Two stimulation protocols, RA and RE, were used to determine whether these features of natural activation had an effect on the SRS-force relationship. No statistically significant differences were found in the SRS-force relationship measured using these protocols, suggesting that motor unit type has a small, if any, effect on MG muscle SRS. The lack of difference between the two electrical stimulation protocols also suggests that SRS

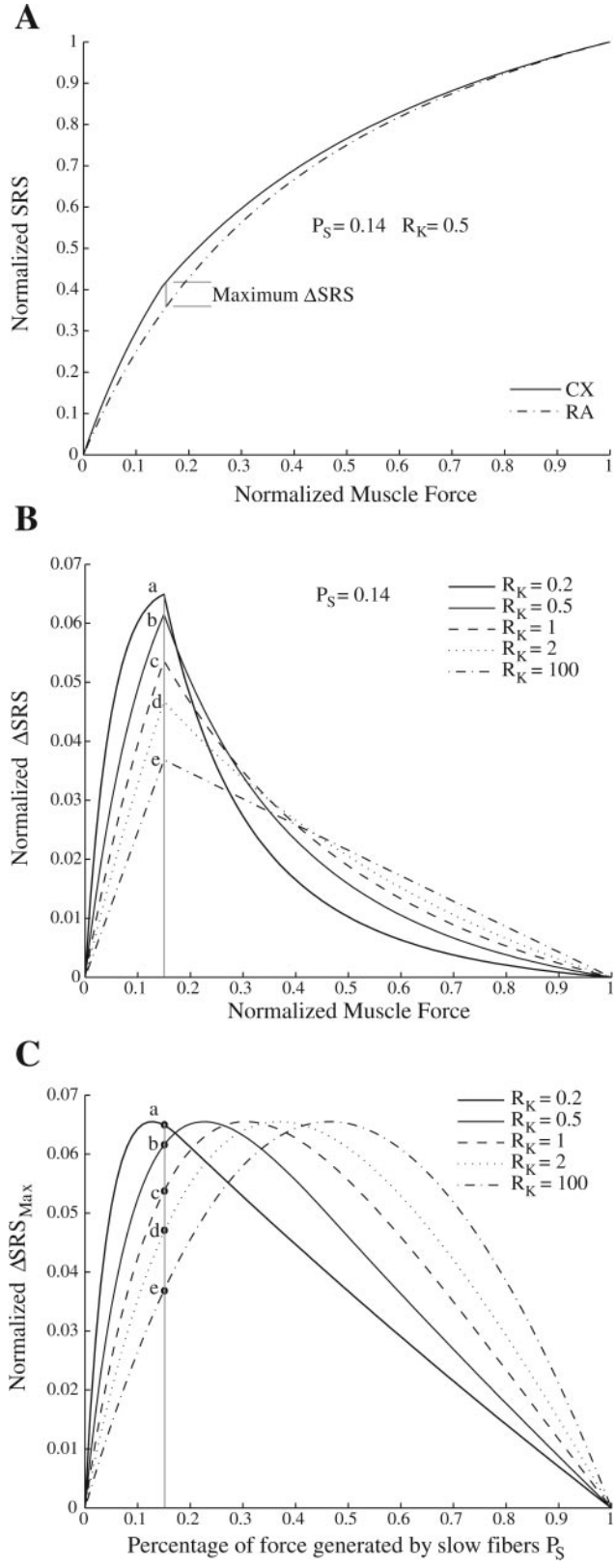

Fig. 6. Model simulation results. *A*: normalized SRS as a function of normalized force for medial gastrocnemius (MG) muscle [percentage of total force generated by slow-twitch muscle (P_S) and ratio of K_T to maximum stiffness (R_K)]. Maximum difference between CX and RA protocols occurs at 14% of total force. *B*: normalized ΔSRS as a function of normalized force for different R_K at $P_S = 0.14$. A stiffer tendon actually decreases normalized ΔSRS *C*: normalized ΔSRS_{max} for each combination of R_K and P_S. Data points *a*–*e* correspond to peak values on curves in *B*.

depends primarily on muscle force, and not on the number of motor units or the firing rates of those motor units. This is the first study to evaluate these effects within the same muscle. The modeling results support and generalize these observations. When the SRS-force relationship is normalized by the maximum SRS, little difference is expected in the SRS-force relationship due to recruitment of different motor unit types. Thus the SRS-force relationship of a muscle must depend primarily on the structural features of a muscle, rather than on its motor unit composition or its activation patterns. These results have important implications for estimation of the SRS-force properties of muscles with varying architectures and, ultimately, how these architectures contribute to the stiffness properties of a limb (16).

Effect of motor unit type and recruitment order on SRS. Although no significant differences in SRS were observed across the population of tested animals, there was a trend toward increased SRS at low forces when the muscles were activated using the CX protocol. This trend is consistent with studies of single fibers and motor units demonstrating that slow-twitch fibers are stiffer than fast-twitch fibers (14, 17), since slow-twitch fibers are recruited first in the CX protocol and last in the electrical stimulation protocols. Thus the SRS-to-force ratio should be higher at low forces. However, this difference is small. As shown in Fig. 2, on the basis of the nonlinear fitting results, the estimated maximum difference in SRS between the CX and the RA protocol is $<10\%$; across the population, this difference dropped to 4%.

The proportion of force contributed by all slow-twitch fibers during normal recruitment has not been verified. The MG muscle has been shown to have 25% type S fibers, with a cross-sectional area of 14% (3). If the specific tension is constant between fast- and slow-twitch fibers, slow-twitch fibers should contribute $\leq 14\%$ of total isometric muscle force. It is unlikely that all type S units are fully recruited before type F motor units are activated; rather, it has been estimated that, in the MG muscle, slow-twitch fibers contribute $\sim 5\%$ of maximal MG force before fast-twitch fibers are recruited. Thus the model in Fig. 6 probably overestimates the difference between the RE and the RA protocol. There is no evidence in cat MG muscle that slow-twitch fibers are shorter than fast-twitch fibers (23), so fiber length will not contribute to the difference in stiffness.

Our simulation results also confirmed that the effect of motor unit recruitment order is small, even in muscles with higher force contributions from slow-twitch fibers and stiffer tendons (Fig. 6*C*). The largest normalized difference in SRS between the CX and the RA protocol was estimated to be $<7\%$ across a wide range of muscle architectures. The proportion of force contributed by slow-twitch fibers only determines the force level at which the largest effect of motor unit recruitment order is expected. ΔSRS_{max} remains nearly constant over a range of simulated tendon stiffnesses. This reflects the fact that these values are normalized by the total muscle-tendon stiffness at maximal activation. The magnitude of ΔSRS does increase with higher tendon stiffness ratios. However, because the corresponding maximal stiffness also increases, the relative effect remains similar.

If it is assumed that the simulation results are accurate, the small difference between CX activation and electrical stimulation, coupled with the experimental variability seen in Fig. 3, suggests that a difference in stiffness between fast- and slow-twitch fibers exists but did not reach statistical significance. However, the experimental results and the simulation suggest that the difference is small enough that it need not be incorporated into models used to understand the stiffness properties of a limb.

Effect of stimulation rate on SRS. No difference was observed between the two electrical stimulation protocols, RA and RE, suggesting that firing rate does not have a substantial effect on SRS. Hence, it did not matter whether the number of attached cross bridges in the muscle was increased by the firing rate (increasing the firing rate of all the ventral roots branches) or activation of more muscle fibers (stimulating additional ventral root branches). Since the SRS-to-force ratio has been shown to change during a twitch (25), the SRS-to-force ratio might vary at low stimulation rates. However, at least with the asynchronous protocol used here, a significant difference was not observed.

No differences in SRS between RA and RE activation. No difference in SRS was observed between the two electrical stimulation protocols, RA and RE, even though they might stretch the common tendon differently. During RA activation, all the muscle fibers are partially active compared with RE coding, where some of the fibers are fully active and some are inactive, possibly resulting in inhomogeneous strain in the aponeurosis and tendon. Proske and Morgan (19) showed in cat soleus muscle that when the tension is $>20\%$ of the maximum muscle force, strain at the end of the tendon was uniform. Thus the cross-linking between collagen fibers in the aponeurosis and tendon may minimize the inhomogeneities and result in similar SRS.

Effect of passive structures on SRS. The model of SRS used in this study assumes that the tendinous structures can be modeled as a single structural element in series with the muscle fibers. This is an obvious simplification of muscle-tendon architecture. There is a stiffness associated with each active fiber that can contribute to the net SRS. Significant compliance in the force transmission within individual fibers or at the interface between these fibers and the external tendon would decrease SRS when only a few fibers are active. This decrease would arise from a reduction in the net stiffness of the passive elements (K_T) connected in series with the active fibers, especially when muscle force is low (19). However, this was not observed in our data. There were no significant differences in the SRS measured during the RA and RE protocols, suggesting that the stiffnesses of each muscle fiber do not act independently. This result may arise from the dispersion of motor unit fibers throughout the muscle (3) and from the extracellular matrix connecting these fibers (27, 28). Significant force transmission through this matrix (26) may reduce the influence of individual fibers on the net passive stiffness and allow the simplified model used in this study to characterize the net SRS of whole muscle.

Another simplification of the present model is that the tendon was modeled as a linear elastic element, in contrast to the many studies demonstrating that the stress-strain relationship of a tendon is nonlinear (5, 11, 12). Nonetheless, the simplified assumption worked well for all data sets. This is likely due to two factors. *1*) At and beyond L_o, the tendon operates beyond the toe region of its stress-strain curve, and its stiffness is fairly constant. *2*) At low forces, the muscle fibers are relatively compliant and, therefore, dominate the whole

muscle SRS. This was observed in the sensitivity analysis (Fig. 5), where it was shown that the sensitivity to K_T was close to or at zero for low muscle forces. This is exactly where the tendon would be in the toe region of its stress-strain curve. Only when significant force is developed does the SRS become more sensitive to K_T than β. By that point, the tendon is likely to be in its linear elastic region. For the cat MG muscle, SRS became more sensitive to changes in K_T beyond ~40% of maximal muscle force, but this point will almost certainly vary across different muscles.

Conclusions. Our experimental findings show that recruitment and firing rate are not substantial factors in determining the SRS of cat MG muscle. Furthermore, the stiffness of the passive muscle structures, connected in series with the muscle fibers, dominates MG muscle SRS at larger muscle forces. A simple model of recruitment is consistent with these experimental results. Hence, although differences in motor unit type are essential for determination of some contractile properties of a muscle, it is the fiber organization and the material properties of the connective tissues that are most critical for determining the initial forces generated in response to external perturbations of muscle length. Appropriate characterization of these properties may allow SRS to be modeled for a variety of muscles with a range of architectures.

GRANTS

This work was supported by National Institute of Arthritis and Musculoskeletal and Skin Diseases Grant R01-AR-041531. E. J. Perreault was supported by National Institute of Child Health and Human Development Grant K25-HD-044720.

REFERENCES

1. **Ariano MA, Armstrong RB, Edgerton VR.** Hindlimb muscle fiber populations of five mammals. *J Histochem Cytochem* 21: 51–55, 1973.
2. **Bennett MB, Ker RF, Dimery NJ, Alexander RM.** Mechanical properties of various mammalian tendons. *J Zool Lond* 209: 537–548, 1986.
3. **Burke RE.** Motor units: anatomy, physiology, and functional organization. In: *Handbook of Physiology. The Nervous System. Motor Control*. Bethesda, MD: Am. Physiol. Soc., 1981, sect. 1, vol. II, p. 345–422.
4. **Clark BD, Dacko SM, Cope TC.** Cutaneous stimulation fails to alter motor unit recruitment in the decerebrate cat. *J Neurophysiol* 70: 1433–1439, 1993.
5. **Fung YC.** Elasticity of soft tissues in simple elongation. *Am J Physiol* 213: 1532–1544, 1967.
6. **Gregory JE, Luff AR, Morgan DL, Proske U.** The stiffness of amphibian slow and twitch muscle during high speed stretches. *Pflügers Arch* 375: 207–211, 1978.
7. **Hunter IW, Kearney RE.** Dynamics of human ankle stiffness: variation with displacement amplitude. *J Biomech* 15: 753–756, 1982.
8. **Huyghues-Despointes CM, Cope TC, Nichols TR.** Intrinsic properties and reflex compensation in reinnervated triceps surae muscles of the cat: effect of activation level. *J Neurophysiol* 90: 1537–1546, 2003.
9. **Joyce GC, Rack PMH, Westbury DR.** The mechanical properties of cat soleus muscle during controlled lengthening and shortening movements. *J Physiol* 204: 461–474, 1969.
10. **Kirsch RF, Boskov D, Rymer WZ.** Muscle stiffness during transient and continuous movements of cat muscle: perturbation characteristics and physiological relevance. *IEEE Trans Biomed Eng* 41: 758–770, 1994.
11. **Lanir Y.** Structure-function relations in mammalian tendon: the effect of geometrical nonuniformity. *J Bioeng* 2: 119–128, 1978.
12. **Lieber RL, Leonard ME, Brown CG, Trestik CL.** Frog semitendinosis tendon load-strain and stress-strain properties during passive loading. *Am J Physiol Cell Physiol* 261: C86–C92, 1991.
13. **Lin DC, Rymer WZ.** Mechanical properties of cat soleus muscle elicited by sequential ramp stretches: implications for control of muscle. *J Neurophysiol* 70: 997–1008, 1993.
14. **Malamud JG, Godt RE, Nichols TR.** Relationship between short-range stiffness and yielding in type-identified, chemically skinned muscle fibers from the cat triceps surae muscles. *J Neurophysiol* 76: 2280–2289, 1996.
15. **Morgan DL.** Separation of active and passive components of short-range stiffness of muscle. *Am J Physiol Cell Physiol* 232: C45–C49, 1977.
16. **Perreault EJ, Kirsch RF, Crago PE.** Multijoint dynamics and postural stability of the human arm. *Exp Brain Res* 157: 507–517, 2004.
17. **Petit J, Filippi GM, Emonet-Denand F, Hunt CC, Laporte Y.** Changes in muscle stiffness produced by motor units of different types in peroneus longus muscle of cat. *J Neurophysiol* 63: 190–197, 1990.
18. **Pollock CM, Shadwick RE.** Relationship between body mass and biomechanical properties of limb tendons in adult mammals. *Am J Physiol Regul Integr Comp Physiol* 266: R1016–R1021, 1994.
19. **Proske U, Morgan DL.** Stiffness of cat soleus muscle and tendon during activation of part of muscle. *J Neurophysiol* 52: 459–468, 1984.
20. **Proske U, Morgan DL.** Tendon stiffness: methods of measurement and significance for the control of movement. *J Biomech* 20: 75–82, 1987.
21. **Proske U, Rack PM.** Short-range stiffness of slow fibers and twitch fibers in reptilian muscle. *Am J Physiol* 231: 449–453, 1976.

21a. **R Development Core Team.** *R: A Language and Environment for Statistical Computing*. Vienna, Austria: R Foundation for Statistical Computing, 2006. http://www.R-project.org. (August 15, 2006).

22. **Rack PM, Westbury DR.** The short range stiffness of active mammalian muscle and its effect on mechanical properties. *J Physiol* 240: 331–350, 1974.
23. **Sacks RD, Roy RR.** Architecture of the hind limb muscles of cats: functional significance. *J Morphol* 173: 185–195, 1982.
24. **Sandercock TG, Heckman CJ.** Whole muscle length-tension properties vary with recruitment and rate modulation in areflexive cat soleus. *J Neurophysiol* 85: 1033–1038, 2001.
25. **Schoenberg M, Wells JB.** Stiffness, force, and sarcomere shortening during a twitch in frog semitendinosus muscle bundles. *Biophys J* 45: 389–397, 1984.
26. **Street SF.** Lateral transmission of tension in frog myofibers: a myofibrillar network and transverse cytoskeletal connections are possible transmitters. *J Cell Physiol* 114: 346–364, 1983.
27. **Thornell LE, Price MG.** The cytoskeleton in muscle cells in relation to function. *Biochem Soc Trans* 19: 1116–1120, 1991.
28. **Trotter JA, Richmond FJR, Purslow PP.** Functional morphology and motor control of series-fibered muscle. *Exerc Sport Sci Rev* 23: 167–213, 1995.
29. **Walmsley B, Proske U.** Comparison of stiffness of soleus and medial gastrocnemius muscles in cats. *J Neurophysiol* 46: 250–259, 1981.